Design and Discovery of MRTX0902, a Potent, Selective, and Orally Bioavailable SOS1 Inhibitor

Abstract LB505

John M. Ketcham, David M. Briere, Aaron C. Burns, James G. Christensen, Robin J. Gunn, Jacob R, Haling, Anthony Ivetac, Shilpi Khare, Jon Kuehler, Svitlana Kulyk, Jade Laguer, John D. Lawson, Krystal Moya, Natalie Nguyen, Peter Olson, Lisa Rahbaek, Christopher R. Smith, Niranjan Sudhakar, Nicole C. Thomas, Darin Vanderpool, Xiaolun Wang, Matthew A. Marx. Mirati Therapeutics, San Diego, CA*

Background

- Activating mutations of KRAS lead to hyperactivation and aberrant signaling within the MAPK pathway[1,2]
- Many of these mutations are single codon mutations (G12, G13, Q61, etc.) and are the most common driver mutations in human cancers[1,2]
- The Son of Sevenless (SOS) protein is a guanine nucleotide exchange factor (GEF) that facilitates the ability of KRAS to turnover from its GDP-loaded “off” state to its GTP-loaded “on” state[3,4]
- Two homologs of SOS exist (SOS1 and SOS2) that impart GEF activity onto KRAS, however, only SOS1 is involved in the negative feedback loop of the KRAS pathway[5,6]
- Functional genomic screens have identified cancer cell lines addicted to KRAS signaling that are particularly sensitive to genetic perturbation of SOS1[7]
- Gain-of-function mutations of SOS1 are reported in Noonan’s syndrome and hereditary gingival fibromatosis (HGF) and are less prevalent in human cancers[4]
- With the promising clinical activity of our KRAS^{G12C} inhibitor adagrasib (**MRTX849**), a combination approach with a SOS1 inhibitor could help shift KRAS^{G12C} into the adagrasib-susceptible GDP-loaded state
- Additionally, SOS1 inhibition can be an indirect approach to targeting other KRAS mutant-driven cancers

Role of SOS1 in the RAS/MAPK Pathway

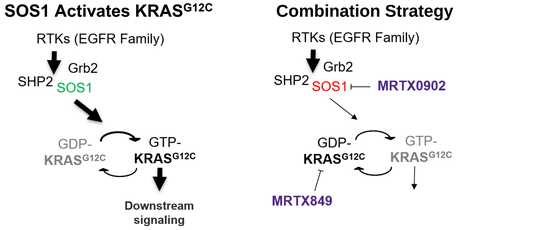

Designing a New Class of SOS1 Inhibitors

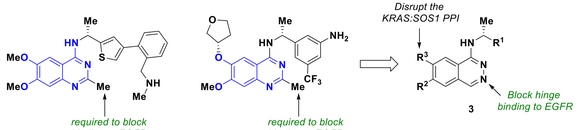

1, BAY-293
KRAS^{G12C}:SOS1^{cat} Interaction Assay IC_{50} = 21 nM

2, BI-3406
SOS1 K_D (SPR) = 3 nM

3

- 2-Me quinazolines have been the primary focus of SOS1 inhibitor design[8]
- Newly designed phthalazine scaffold can provide distinct physicochemical properties when compared to previously reported inhibitors
- Phthalazines block EGFR binding without the need for 2-methyl substituent

Initial SAR for Simplified Phthalazines

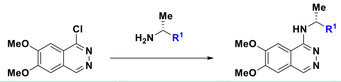

Compound	R^1	SOS1 Binding K_i (nM)	MKN1 Cell IC_{50} (nM)[a]	EGFR IC_{50} (nM)
4		637	>10000	>10000
5		76	>10000	>10000
6		52	958	>10000
7		2049	>10000	>10000
8		13	378	>10000
9		3.9	165	>10000

[a]In Cell Western Assay measuring pERK

C4-Methyl Blocks AO Metabolism

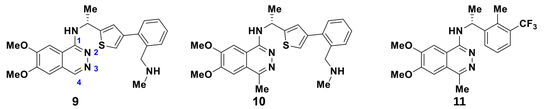

9 **10** **11**

Compound	SOS1 Binding K_i (nM)	MKN1 Cell IC_{50} (nM)	$t_{1/2}$ (min) human liver S9	$t_{1/2}$ (min) human liver S9 + 25 µM Raloxifene
9	3.9	165	14	>180
10	0.54	249	>180	>180
11	2.6	195	>180	>180

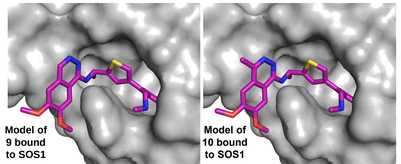

- C4-methyl blocks AO metabolism without loss in binding and cellular potency

Representative SAR leading to MRTX0902

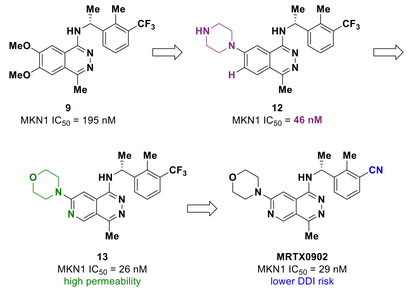

9
MKN1 IC_{50} = 195 nM

12
MKN1 IC_{50} = **46 nM**

13
MKN1 IC_{50} = 26 nM
high permeability

MRTX0902
MKN1 IC_{50} = 29 nM
lower DDI risk

- Deletion of the C6-methyl ether and installation of a C7-piperazine resulted in **increased cellular potency**
- Combination of the azaphthalazine core with a C7-morpholine led to **high permeability**
- Replacing the 3-CF_3 phenyl substituent with a 3-cyano resulted in **lower DDI risk**

Co-Crystal Structure of SOS1:MRTX0902

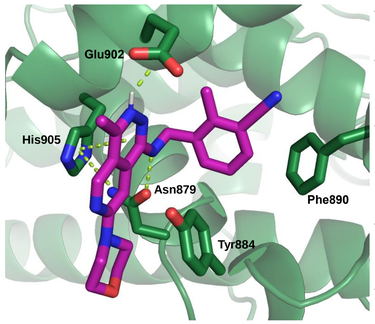

- Phthalazine core shares π-stacking interaction with His905
- N-H from the C1-benzyl amine substituent creates a crucial hydrogen bond with Asn879
- Chiral α-methyl on benzylic amine fills a small hole and facilitates a turn into the hydrophobic back pocket, positions phenyl group for an edge-to-face interaction with Phe890
- Protonated N3-nitrogen within the phthalazine core makes a salt bridge with the carboxylate of Glu902
- C7-morpholine pushes into the KRAS:SOS1 interface and blocks the protein-protein interaction

MRTX0902 In Vitro Profile

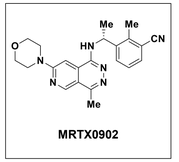

MRTX0902

Assay	Activity
SOS1 Binding K_i (nM)	2
MKN1 Cell IC_{50} (nM)	29
SOS2 KRAS WT GDP Exchange IC_{50} (nM)	>10000
EGFR IC_{50} (nM)	>10000
MW / clogP / PSA	388.5 / 3.4 / 86.9

MRTX0902 Pharmacokinetic Profile

- **MRTX0902** displays clearance less than 22% of hepatic blood flow and bioavailability of 38-83% across species

Compound	mouse Cl_{total} (mL/min/kg) | Vd_{ss} (L/kg) | $t_{1/2}$ (h) | F (%)[a]	rat Cl_{total} (mL/min/kg) | V_{ss} (L/kg) | $t_{1/2}$ (h) | F (%)[b]	dog Cl_{total} (mL/min/kg) | V_{ss} (L/kg) | $t_{1/2}$ (h) | F (%)[c]
MRTX0902	4.4 | 0.28 | 1.3 | 69	14.6 | 0.28 | 0.62 | 83	7.6 | 0.48 | 0.86 | 38

[a]IV Dosing: 3 mg/kg, PO Dosing: 30 mg/kg [b]IV Dosing: 1 mg/kg, PO Dosing: 10 mg/kg [c]IV Dosing: 2 mg/kg, PO Dosing: 10 mg/kg

- PO dosing (100 mg/kg) of **MRTX0902** in female CD-1 mice (n=3) results in CSF exposures that exceed the cellular IC_{50} (29 nM) for up to 8 hours

Time (h)	Mean Brain Conc. (ng/g)	Mean CSF Conc. (nM)
1	1388	81
8	388	36

MRTX0902 with MRTX849 Results in Complete Regression in KRAS^{G12C} MIA PaCa-2 Model

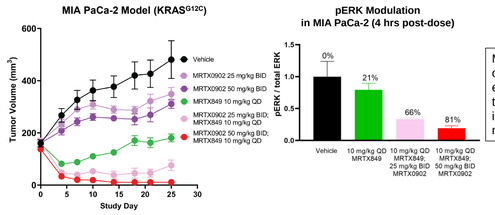

MRTX0902 + MRTX849 combo leads to enhanced inhibition of the MAPK pathway as indicated by pERK1/2 modulation

Mice bearing MIA PaCa-2 tumors were treated with Vehicle PO QD, MRTX849 at 10mg/kg PO QD, MRTX0902 at 25 and 50 mg/kg bid, or the combination for the duration of the study. Data shown as average tumor volume +/- SEM, or individual tumor volumes, n=5/group. *2 tumor free animals.

Conclusions

- Through rational design, we have discovered **MRTX0902** – a potent, selective, and orally bioavailable inhibitor of SOS1 that is brain penetrant
- **MRTX0902** in combination with our KRAS^{G12C} inhibitor **MRTX849** yields enhanced MAPK pathway inhibition and complete tumor regression in the KRAS^{G12C} MIA PaCa-2 Model
- **MRTX0902** is currently in IND-enabling studies, planned submission in 2H 2022

Acknowledgements and References

1. Bos, J. L. *Cancer Res* **1989**, *49*, 4682-4689.
2. Simanshu, D. K.; Nissley, D. V.; McCormick, F. *Cell* **2017**, *170*, 17−33.
3. Boriack-Sjodin, P. A.; Margarit, S. M.; Bar-Sagi, D.; Kuriyan, J. *Nature* **1998**, *394*, 337−343.
4. Kessler, D.; Gerlach, D.; Kraut, N.; McConnell, D. B. *Curr. Opin. Chem. Biol.* **2021**, *62*, 109-118.
5. Rozakis-Adcock, M.; Geer, P.; Mbamalu, G.; Pawson, T. *Oncogene* **1995**, *11*,1417–1426.
6. Corbalan-Garcia, S.; Yang, S.; Degenhardt, K.; Bar-Sagi, D. *Mol. Cell Biol.* **1996**, *16*, 5674–5682.
7. Jeng, H.-H.; Taylor, L. J.; Bar-Sagi, D. *Nat. Commun.* **2012**, *3*, 1168.
8. Kessler, D.; Gerlach, D.; Kraut, N.; McConnell, D. B. *Curr. Opin. Chem. Biol.* **2021**, *62*, 109-118.

- We would like to thank our collaborators at WuXi AppTec: Feng Zhao, Xiaodong Xu, Xing Su, Rongfeng Zhao, Shaojun Song, Wenbing Ruan, Wenchao Fei, Yunting Xu, Binbin Tian, and Huihui Li.
- The x-ray crystallography work is based upon research conducted at the Northeastern Collaborative Access Team beamlines